Solidification and dynamic wetting:

Shikhmurzaev, Yulii D.

DOI:
10.1063/5.0054431

Document Version
Publisher's PDF, also known as Version of record

Citation for published version (Harvard):
Shikhmurzaev, YD 2021, 'Solidification and dynamic wetting: A unified modeling framework', *Physics of Fluids*, vol. 33, no. 7, 072101. https://doi.org/10.1063/5.0054431

Solidification and dynamic wetting: A unified modeling framework

Cite as: Phys. Fluids **33**, 072101 (2021); https://doi.org/10.1063/5.0054431
Submitted: 18 April 2021 • Accepted: 08 June 2021 • Published Online: 01 July 2021

Yulii D. Shikhmurzaev

Physics of Fluids ARTICLE scitation.org/journal/phf

Solidification and dynamic wetting: A unified modeling framework

Cite as: Phys. Fluids **33**, 072101 (2021); doi: 10.1063/5.0054431
Submitted: 18 April 2021 · Accepted: 8 June 2021 ·
Published Online: 1 July 2021

Yulii D. Shikhmurzaev[a)]

AFFILIATIONS

School of Mathematics, University of Birmingham, Birmingham B15 2TT, United Kingdom

[a)]Author to whom correspondence should be addressed: y.d.shikhmurzaev@bham.ac.uk

ABSTRACT

A conceptual and mathematical framework for the singularity-free modeling of non-equilibrium solidification/melting and non-isothermal dynamic wetting is developed where both processes are embedded into a broader class of physical phenomena as particular cases. This allows one to consider problems describing fluid flows with phase transitions and dynamic wetting occurring independently or interactively in a regular conceptually consistent way without *ad hoc* assumptions. The simplest model formulated on the basis of this approach explains, at this stage qualitatively, the arrest of the moving contact line observed experimentally in the impact and spreading of a molten drop on a cold substrate. The classical Stefan problem and the model of isothermal dynamic wetting as an interface formation process are recovered as limiting cases.

I. INTRODUCTION

Dynamic wetting and solidification come together in a number of situations, both in natural phenomena and in various technologies. Among the latter is the process of additive manufacturing, where, in one of its many variants, a 3D solid structure is built by successive deposition and subsequent solidification of drops of different materials.[1,2] A similar process is involved in the manufacturing of electronic circuits and some other technologies.[3]

From a practical viewpoint, one of the main challenges is predicting and, technologically, controlling the size of the drop's base on its solidification. Together with a related problem of predicting the final shape of the solidified drop, this issue is at the core of the whole process of building 3D structures. All aspects of the drop deposition and solidification depend also on other factors, from roughness and/or chemical heterogeneity as well as deformability of the substrate to evaporation of the liquid forming the drop and the dynamics and chemical properties of the ambient gas.

From the viewpoint of mathematical modeling, there is a hierarchy of effects in this complex phenomenon, and the main elements are (i) dynamic wetting, which, in the drop spreading context, creates the area of contact between the liquid and the solid, and (ii) solidification responsible for the final outcome of the process. This suggests examining an idealized situation where the solid substrate is smooth chemically homogeneous and non-deformable, while the ambient gas is inert and dynamically passive, with the evaporation-condensation effects negligible on the timescale considered. The material of the substrate can be different from that of the liquid, in which case for simplicity it can be taken as chemically inert with respect to the liquid, or it can be of the same kind. In both cases, the key question is whether dynamic wetting and solidification are entangled inseparably or, as in Fig. 1, initially occur as independent phenomena which at a later stage interact. The answer to this question determines the modeling scheme within which particular mathematical models are then to be formulated.

An experimentally observed feature that can be used as a test for the modeling scheme is the arrest of the moving contact line.[4–8] Descriptively, the essence of this phenomenon is that a molten drop on a cold substrate spreads as if in isothermal conditions until the spreading suddenly stops, and then, the drop simply solidifies with its base not expanding anymore. The spreading phase is not affected by the substrate undercooling,[8] whereas the time to the arrest and the maximum size of the drop's base decrease as the substrate undercooling increases.[4,5,8]

The first modeling scheme to describe this effect was proposed by Schiaffino and Sonin[6,9] who, prompted by their experiment,[6] which dealt with forced rather than spontaneous spreading, suggested that the whole of the drop's base solidifies as it is expanding; that is, the moving contact line is also the edge of the solidification front. Then, according to Refs. 6 and 9, the arrest of the contact line occurs when the slope of the solidification front at the contact line/edge coincides

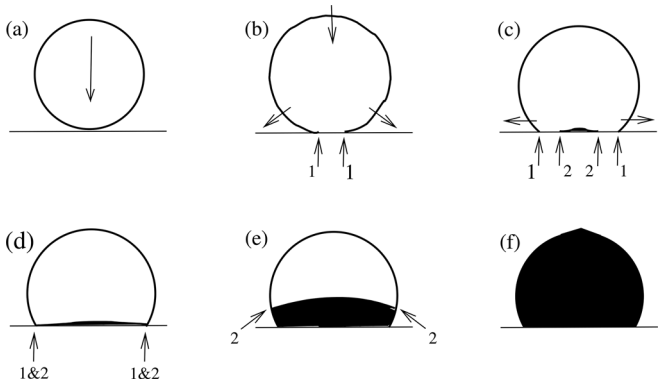

FIG. 1. A sketch of the droplet spreading and solidification process. (a) the onset of the process, $t = 0$; (b) the geometric/kinematic stage of spreading where the size of the drop's base expands $\propto \sqrt{t}$; (c) the onset and initial dynamics of solidification; (d) the arrest of the contact line; (e) solidification with a fixed base; (f) the end of the process. The numbered arrows point at the liquid/gas/substrate contact line (1) and the edge of the solidification front (2).

with the slope of the free surface. A similar modeling scheme with a solidifying base but a different criterion for the arrest has been used in Ref. 7.

An alternative scheme was proposed by Tavakoli *et al.*[4] who assumed that solidification occurs not everywhere on the expanding base of the drop but starts from the moving contact line. In this scheme, the contact line is assumed to be carrying with it a block of "ice" (already solidified liquid) and stops moving when this block reaches a certain critical size.

Thus, both schemes regard dynamic wetting and solidification as inseparable.

These schemes of the process have been, first, questioned by de Ruiter *et al.*[5] who observed that "as shown by both the spreading radius and the contact angle data, the drop dynamics prior to arrest is experimentally indistinguishable from isothermal spreading without solidification" so that "the motion of the contact line is completely unaffected by the cooling prior to the arrest." This would not have been the case should the flow geometry near the contact line continuously vary due to the solidification front having its edge at the contact line and increasing its slope, as in Refs. 6, 7, and 9, not to mention should the contact line be carrying a block of ice with it as in Ref. 4. Moreover, the latest experiments,[10,11] where the solidification front was actually visualized, have shown that dynamic wetting and the propagation of the solidification front are separate processes and the arrest of the contact line happens once they interact. Schematically, the process is shown in Fig. 1.

This scheme, which we will use below, is also consistent with the fact that the drop impact onto a solid is followed by the so-called geometric (or kinematic) wetting regime corresponding to the size of the drop's base expanding $\propto \sqrt{t}$, where t is the time measured from the moment of impact. In this regime, the speed at which the base initially expands is infinite as it is determined entirely by the speed of impact and the geometry of the two smooth surfaces brought into contact, while solidification is governed by physical factors, and hence, it takes a finite time for it to begin.[12]

Thus, dynamic wetting and solidification appear as separate processes and, in essence, the scheme sketched in Fig. 1 involves *two* "moving contact lines" with the second one being the leading edge of the solidification front whose propagation along the substrate is controlled mainly by the solidification dynamics and the associated thermal processes. The spreading of the drop is arrested when the edge of the solidification front catches up with the contact line [Fig. 1(d)] and, not being able to propagate sideways anymore, it climbs up the free surface.

The modeling scheme sketched in Fig. 1 makes it necessary to embed dynamic wetting and solidification/melting into a unifying modeling framework encompassing both of these processes so that each of them separately and their interaction could be described without any *ad hoc* adjustments and arbitrary criteria.

In this work, we develop the required framework and show that it covers the whole range, from the classical Stefan problem for equilibrium solidification and its generalization to a non-equilibrium case to the model of dynamic wetting as an interface disappearance-formation process which is, as reviewed in Ref. 13, uniquely able to describe both spontaneous and forced spreading without prescribing any dependence of the dynamic contact angle as a function of the contact-line speed.

The paper is organized as follows. Section II recapitulates the Stefan problem and points out why it does not allow one to describe the propagating edge of the solidification front. In Sec. III, the model of an out-of-equilibrium interface as a two-dimensional surface phase is derived in sufficient detail to make the derivation easily reproducible. In Sec. IV, we show how it reduces to the Stefan model and the model for isothermal dynamic wetting as limiting cases. Section V specifies what the edge of the solidification front is in terms of the developed model in the situations where the substrate is of the same material as the liquid or of a different one and what angle the front makes with the substrate at the edge. In Sec. VI, the phenomenon of the arrest of the moving contact line is qualitatively explained. Finally, in Sec. VII, we put the developed framework into a broader modeling context from the continuum mechanics and physical chemistry perspective and discuss some of the assumptions made in the derivation of the simplest model and possible ways of its generalization.

II. THE STEFAN PROBLEM AND THE EDGE OF SOLIDIFICATION FRONT

Consider the propagation of a solidification front as it is modeled in terms of the Stefan problem[14] which, for generality, we will couple with the fluid-mechanical problem. Let $f(\mathbf{r}, t) = 0$ describe the current location of the solidification front, where $\mathbf{r}$ is the position vector and t is the time, such that $\mathbf{n} = \nabla f/|\nabla f|$ is a unit normal to the solidification front pointing into the liquid. The bulk parameters of the liquid ($f > 0$) and the solid into which the liquid solidifies ($f < 0$) will be marked with superscript + and –, respectively.

In a differential form, equation $f(\mathbf{r}, t) = 0$ becomes

$$\frac{\partial f}{\partial t} + \mathbf{v}^s \cdot \nabla f = 0, \tag{1}$$

thus introducing the normal component of $\mathbf{v}^s$ as the speed at which the front propagates.

The liquid is assumed to be incompressible so that its velocity $\mathbf{u}^+$, pressure p^+ and, if the process is not isothermal, temperature T^+ satisfy the following equations:

$$\nabla\cdot\mathbf{u}^+=0,\quad \rho^+\left(\frac{\partial\mathbf{u}^+}{\partial t}+\mathbf{u}^+\cdot\nabla\mathbf{u}^+\right)=-\nabla p^++\mu^+\nabla^2\mathbf{u}^+, \tag{2}$$

$$\rho^+c^+\left(\frac{\partial T^+}{\partial t}+\mathbf{u}^+\cdot\nabla T^+\right)=\kappa^+\nabla^2T^+ +\mu^+\left[\nabla\mathbf{u}^+:\nabla\mathbf{u}^++\nabla\mathbf{u}^+:(\nabla\mathbf{u}^+)^*\right], \tag{3}$$

where ρ^+, μ^+, c^+, and κ^+ are the density, viscosity, specific heat, and thermal conductivity of the liquid. These parameters are assumed to be constant and, for simplicity, their possible dependence on temperature neglected. The asterisk in Eq. (3) indicates transposition.

The solid into which the liquid solidifies is modeled as rigid (non-deformable) and, for generality, moving with velocity $\mathbf{u}^-$. Then, the temperature distribution in the solid is described by the heat conduction equation

$$\rho^-c^-\left(\frac{\partial T^-}{\partial t}+\mathbf{u}^-\cdot\nabla T^-\right)=\kappa^-\nabla^2T^-, \tag{4}$$

where $\mathbf{u}^-$ is prescribed/known. For the situation sketched in Fig. 1, $\mathbf{u}^-\equiv 0$.

The number of boundary conditions required at the solidification front is easy to figure out. The fluid mechanical side, that is, Eq. (2), requires three scalar boundary conditions; in standard fluid mechanical problems, these conditions specifying the components of velocity $\mathbf{u}^+$ are the impermeability condition for the normal component of $\mathbf{u}^+$ and the no-slip conditions for its two tangential components. The thermal side, that is, Eqs. (3) and (4), requires—if the location of the liquid–solid interface is known and no phase transition takes place—two conditions, which, in standard thermal problems, are the continuity of temperature and of the normal component of the heat flux. For a moving solidification, front one needs to modify the heat flux condition to account for the latent heat and add one more condition to specify the normal component of $\mathbf{v}^s$, thus making it possible to find f from Eq. (1).

In the Stefan problem, the required six scalar boundary conditions linking the bulk parameters on both sides of the solidification front have the form:

$$\rho^+(\mathbf{u}^+-\mathbf{v}^s)\cdot\mathbf{n}=\rho^-(\mathbf{u}^--\mathbf{v}^s)\cdot\mathbf{n}, \tag{5}$$

$$\mathbf{u}^+_{||}=\mathbf{u}^-_{||}, \tag{6}$$

$$T^+=T^-=T_m, \tag{7}$$

$$(\kappa^+\nabla T^+-\kappa^-\nabla T^-)\cdot\mathbf{n}=H_L\rho^+(\mathbf{u}^+-\mathbf{v}^s)\cdot\mathbf{n}, \tag{8}$$

where the melting temperature T_m is a known constant and H_L is the latent heat of fusion. The subscript $||$ in Eq. (6) denotes the component parallel to the solidification front's surface, that is, $\mathbf{u}_{||}=\mathbf{u}\cdot(\mathbf{I}-\mathbf{nn})$, where $\mathbf{I}$ is the metric tensor. The Stefan problem is typically studied for a quiescent media where the fluid dynamic side is irrelevant/omitted; here, we state it in a general form.

The boundary conditions (1), (5)–(7) do not allow one to describe the propagation of the solidification front with a moving edge [Fig. 1(c)]. Indeed, the local asymptotic analysis near the edge involves, to leading order, Laplace's equations for T^+ and T^- with conditions (7) on the front and the continuity of temperature and of the normal component of the heat flux on the substrate ahead of the edge, and, as mentioned, for example, in Ref. 9, in the solution to this problem the heat fluxes become singular as the edge is approached. This singularity does not allow one to determine the normal component of $\mathbf{v}^s$ from Eq. (8), which involves the fluxes and not their integrals, so that integrability of the fluxes is irrelevant. In this sense, the "moving edge problem" is more demanding than the "moving contact-line problem,"[15] where the issue initially was non-integrability of the shear stress at the contact line and only later the research focus moved to the "dynamic contact-angle problem"; see Ref. 13 for a recent review.

Furthermore, in the Stefan problem applied to the solidification front with an edge [Fig. 1(c)] the heat flux singularity is present even if the solidification front joins the substrate ahead of it smoothly; that is, the "contact angle," should it be measured between the solidification front and the substrate behind it, is zero. This is a direct consequence of the discontinuity in the boundary conditions as here we have a prescribed temperature T_m for both bulk phases on one part of the boundary and the continuity of temperature and the normal components of the heat fluxes on the other with different thermal conductivities κ^+ and κ^-. Then, the fluxes go to infinity as one approaches the point of discontinuity in the boundary conditions from either side.

Thus, the scheme sketched in Fig. 1 requires that the temperature distribution near the edge of the solidification front is modeled in a singularity-free way and, furthermore, that the model is formulated in the same conceptual framework as the one used for the moving contact-line problem so that the description of the whole flow of the type sketched in Fig. 1 is conceptually self-consistent. Given that, as shown in Ref. 13, the only adequate solution to the moving contact-line problem is the one that embeds it as a particular case in a generic class of fluid flows with forming/disappearing interfaces,[16] it is the development of this framework to account for thermal effects and phase transitions that should be looked into to address the moving edge problem.

III. UNIFIED MODELING FRAMEWORK

A. Sharp interface and surface variables: Continuum limit vs "dividing surface"

Conceptually, there are two ways of introducing sharp interfaces as two-dimensional "surface phases" separating the "bulk phases" where partial differential equations of continuum mechanics operate. Both ways come down to largely the same mathematics describing conservation laws but differ substantially with regard to the physics involved in the closure of the model, that is, constitutive equations and equations of state, which ultimately determine what physical phenomena the model can describe.

The first approach is where, following Gibbs,[17] the interface as a two-dimensional surface phase is introduced by using an artificial construct known as the "dividing surface." This is assumed to be a surface passing somewhere inside the interfacial layer and thus dividing the continuum medium into two distinct bulk phases. Then, the bulk distributions of parameters on each side of the dividing surface are extrapolated up to this surface, and the "excess" quantities are attributed to the dividing surface as parameters characterizing the interface as a surface phase. Notably, this approach presumes that there is some smooth distribution of the bulk parameters to be extrapolated but

does not actually consider the continuum limit, which introduces these distributions and what it implies. The dividing surface approach has been used in numerous works, reviewed, for example, in Refs. 18 and 19, focusing primarily on the derivation of new models of increasing complexity albeit typically without the closure relations, which might have made these models usable.

An alternative approach stems from acknowledging that the very notions of the "bulk phases," "interfaces" as surfaces separating the bulk phases, "contact lines" as the lines of intersection of interfaces appear as the leading-order approximation in the continuum (or thermodynamic) limit, which can be defined as the ratios of molecular-to-macroscopic length and time scales going to zero. This limit simultaneously introduces smooth distributions of the bulk parameters subject to the partial differential equations operating there and collapses what physically are interfacial layers between bulk phases into sharp "interfaces." In other words, in this approach both bulk phases and sharp interfaces between them appear naturally and simultaneously as a result of the continuum approximation and hence the interfaces retain all physical properties of the interfacial layers which they represent and whose thickness, being on a molecular scale, is, to leading order, simply neglected compared with the length scale characterizing the bulk on which the resulting model is expected to describe physical phenomena.

Both approaches introduce surface parameters characterizing the interface as a two-dimensional surface phase, and the difference comes in their physical interpretation and hence in the closure of the model where this interpretation becomes involved. For example, if the density distribution shows no "excess" in the interfacial layer, then the dividing surface approach does not include this parameter in the description of the surface phase and treats the latter as massless, for example, Ref. 20, but somehow endows it with other surface properties, for example, temperature. More generally, there are no reasons to expect that the "excess" quantities will obey the same thermodynamic laws as the quantities with respect to which this excess is considered or indeed any laws. This and some other issues with the dividing surface approach come essentially from its artificiality as a conceptually geometric construct imposed on top of a descriptively continuous picture of the parameter distributions, and they go deeper than the much debated issue of where to locate the dividing surface[19,21] and additional artificial constructs intended to make the resulting models independent of its location.[22]

By contrast, the continuum-limit-based approach recognizes that a sharp interface is merely a representation of an interfacial layer of a finite thickness on a macroscopic length scale where this thickness is negligible. Then, all parameters characterizing the interfacial layer can be ascribed to the interface as "surface parameters," that is, parameters per unit area rather than per unit volume. These parameters can be seen as integrals across the layer of the corresponding distributions. As a result, neither the paradox of a massless interface endowed with its own temperature nor any other contentious issue regarding the dividing surface approach even arises as the interface appears merely as a two-dimensional representation of a three-dimensional system.

Importantly, the continuum-limit-based approach also resolves the issues raised against the modeling of interfaces as layers of a finite thickness,[23] which is often seen as the only alternative to the dividing surface approach[18,19] and where the thickness of the layer and the location of its boundaries are also an issue: the continuum limit collapses interfacial layers into sharp interfaces without specifying the exact thickness of the former so that the formal geometric consideration of interfaces as layers becomes irrelevant, and they become defined via their physics, that is, constitutive equations, equations of state and the parameters these equations involve, rather than their geometry. A discussion of this issue can be found in Ref. 16.

In what follows, we adopt the continuum-limit-based approach and point out where its outcome is at variance with early attempts to describe interfaces with phase transitions in the dividing surface framework.

B. Conservation laws

Consider a solidification front where, in terms of modeling, a viscous incompressible liquid turns into a rigid solid. In the continuum limit, that is, on a length scales large compared with the (molecular-scale) thickness of the layer where the phase transition takes place, the solidification front can be modeled as a sharp interface, a two-dimensional "surface phase" endowed with its own "surface properties." As before, let $f(\mathbf{r},t)=0$ describe the location of the solidification front at time t, so that in the differential form we again have (1), and let $\mathbf{n}=\nabla f/|\nabla f|$ be a unit normal to the front pointing into the liquid.

In order to model the process of solidification in terms of the boundary conditions for the bulk phases, it is convenient to use the mathematical technique developed by Bedeaux *et al.*,[24] which employs the formalism of generalized functions thus by-passing the need to make assumptions, first, specifying the structure of the interfacial transition layer between the bulk phases with the appropriate distributions across it and, second, to make additional assumptions to collapse this structure into averaged "surface properties." At the same time, the mathematical formalism itself has certain implications that have to be addressed when the resulting model is fine-tuned to a particular physical system.

Following Ref. 24, we will, as before, mark the bulk parameters of the liquid ($f>0$) and the solid ($f<0$) with superscripts + and –, respectively, and, where necessary, use the subscript s for the surface parameters.

Introduce two Heaviside functions

$$\theta^+=\begin{cases}1, & f>0\\ 0, & f\le 0\end{cases},\qquad \theta^-=\begin{cases}0, & f\ge 0\\ 1, & f<0\end{cases}$$

and the following normalized delta-function:

$$\delta^s(\mathbf{r},t)=\delta(f(\mathbf{r},t))|\nabla f(\mathbf{r},t)|,$$

where $\delta(f)$ is the standard delta-function. For these functions, we have[24]

$$\nabla\theta^{\pm}=\pm\mathbf{n}\delta^s,\quad \frac{\partial\theta^{\pm}}{\partial t}=\mp\mathbf{v}^s\cdot\mathbf{n}\delta^s,\quad \frac{\partial\delta^s}{\partial t}=-\mathbf{v}^s\cdot\nabla\delta^s. \tag{9}$$

All parameters characterizing the surface phase A^s and the normal $\mathbf{n}$ are defined only on the interface such that their derivatives in the direction normal to the surface are zero, so that

$$\mathbf{n}\cdot\nabla A^s=\mathbf{n}\cdot\nabla\mathbf{n}=0,$$

and, as shown in Ref. 24, if for two-surface quantities A^s and $\mathbf{B}^s$

$$A^s\delta^s + \mathbf{B}^s \cdot \nabla\delta^s = 0, \tag{10}$$

and then, it follows that:

$$A^s = \mathbf{B}^s \cdot \mathbf{n} = 0. \tag{11}$$

Now, we can introduce the density ρ, mass and momentum fluxes $\rho\mathbf{u}$, $\rho\mathbf{uu}$ and the stress tensor $\mathbf{P}$ defined across all three phases:

$$\rho(\mathbf{r},t) = \rho^+(\mathbf{r},t)\theta^+(\mathbf{r},t) + \rho^s(\mathbf{r},t)\delta^s(\mathbf{r},t) + \rho^-(\mathbf{r},t)\theta^-(\mathbf{r},t), \tag{12}$$

$$(\rho\mathbf{u}, \rho\mathbf{uu}) = (\rho^+\mathbf{u}^+, \rho^+\mathbf{u}^+\mathbf{u}^+)\theta^+ + (\rho^s\mathbf{v}^s, \rho^s\mathbf{v}^s\mathbf{v}^s)\delta^s + (\rho^-\mathbf{u}^-, \rho^-\mathbf{u}^-\mathbf{u}^-)\theta^-, \tag{13}$$

$$\mathbf{P} = \mathbf{P}^+\theta^+ + \mathbf{P}^s\delta^s + \mathbf{P}^-\theta^-, \quad \mathbf{u} = \begin{cases} \mathbf{u}^+, & f > 0 \\ \mathbf{v}^s, & f = 0 \\ \mathbf{u}^-, & f < 0 \end{cases}. \tag{14}$$

After substituting expressions (12)–(14) into the mass and momentum balance equations

$$\frac{\partial\rho}{\partial t} + \nabla\cdot(\rho\mathbf{u}) = 0, \quad \frac{\partial\rho\mathbf{u}}{\partial t} + \nabla\cdot(\rho\mathbf{uu}) = \nabla\cdot\mathbf{P}$$

and using (9)–(11), we equate to zero separately coefficients in front of θ^+, θ^-, δ^s and the normal component of the coefficient in front of $\nabla\delta^s$ to obtain the mass and momentum balance equations in the bulk phases and the surface phase. For the latter, this yields

$$\frac{\partial\rho^s}{\partial t} + \nabla\cdot(\rho^s\mathbf{v}^s) = -\rho^+(\mathbf{u}^+ - \mathbf{v}^s)\cdot\mathbf{n} + \rho^-(\mathbf{u}^- - \mathbf{v}^s)\cdot\mathbf{n} \tag{15}$$

and

$$\frac{\partial\rho^s\mathbf{v}^s}{\partial t} + \nabla\cdot(\rho^s\mathbf{v}^s\mathbf{v}^s) + \rho^+\mathbf{u}^+(\mathbf{u}^+ - \mathbf{v}^s)\cdot\mathbf{n} - \rho^-\mathbf{u}^-(\mathbf{u}^- - \mathbf{v}^s)\cdot\mathbf{n} = \nabla\cdot\mathbf{P}^s + \mathbf{n}\cdot(\mathbf{P}^+ - \mathbf{P}^-), \tag{16}$$

$$\mathbf{P}^s\cdot\mathbf{n} = 0. \tag{17}$$

The last equation simply states that the surface stress acts in the plane tangential to the interface.

In a similar way, after substituting the internal energy per unit volume U_v and the heat flux $\mathbf{q}$ in the form

$$U_v = U_v^+\theta^+ + U_v^s\delta^s + U_v^-\theta^-, \quad \mathbf{q} = \mathbf{q}^+\theta^+ + \mathbf{q}^s\delta^s + \mathbf{q}^-\theta^-, \tag{18}$$

in the energy balance equation

$$\frac{\partial}{\partial t}\left(\frac{\rho\mathbf{u}^2}{2} + U_v\right) + \nabla\cdot\left[\mathbf{u}\left(\frac{\rho\mathbf{u}^2}{2} + U_v\right) - \mathbf{P}\cdot\mathbf{n} + \mathbf{q}\right] = 0,$$

and subtracting the equations for kinetic energies of the phases obtained in the usual way; that is, by multiplying the equations of motion by the corresponding velocities, we arrive at the following equation for the internal energy of the surface phase

$$\frac{\partial U_v^s}{\partial t} + \nabla\cdot(\mathbf{v}^sU_v^s) + U_v^+(\mathbf{u}^+ - \mathbf{v}^s)\cdot\mathbf{n} - U_v^-(\mathbf{u}^- - \mathbf{v}^s)\cdot\mathbf{n} + \frac{1}{2}\rho^+(\mathbf{u}^+ - \mathbf{v}^s)^2(\mathbf{u}^+ - \mathbf{v}^s)\cdot\mathbf{n} - \frac{1}{2}\rho^-(\mathbf{u}^- - \mathbf{v}^s)^2(\mathbf{u}^- - \mathbf{v}^s)\cdot\mathbf{n} - \mathbf{P}^s : \nabla\mathbf{v}^s - \mathbf{n}\cdot\mathbf{P}^+\cdot(\mathbf{u}^+ - \mathbf{v}^s) + \mathbf{n}\cdot\mathbf{P}^-\cdot(\mathbf{u}^- - \mathbf{v}^s) + (\mathbf{q}^+ - \mathbf{q}^-)\cdot\mathbf{n} + \nabla\cdot\mathbf{q}^s = 0, \tag{19}$$

and also the equation

$$\mathbf{q}^s\cdot\mathbf{n} = 0, \tag{20}$$

stating that the surface heat flux is directed along the interface.

Equations (15)–(20) are simply conservation laws formally applied to a system with two bulk phases and one surface phase.

C. Thermodynamics of the interface and simplifying assumptions

The use of δ^s in Eqs. (12), (13), and (18) for the density, momentum, and thermal flux formally expanded the class of possible models to include those where the direct effect of the surface phase goes far beyond capillarity. Now, we need to narrow this class down by estimating the magnitude of the terms this expansion brought in for the systems of our interest. The key here is that, if we consider the interfacial layer represented in the continuum limit by the sharp "interface," the densities of mass, momentum, and heat flux varying across it are of the same order as the corresponding bulk variables, while the thickness of this layer in the continuum limit is negligible compared with the length scale characterizing the bulk distributions. Then, one can simplify the equations by neglecting the terms, which, according to the estimates, are proportional to the thickness of the interfacial layer unless their role is magnified by some other factors. The latter is the case for the surface tension where the negligible thickness of the interfacial layer is compensated by singularly strong (intermolecular) forces of non-hydrodynamic origin from the bulk phases. The use of the estimates similar to what we are going to do can be found, for example, in Ref. 25 albeit without a reference to the continuum limit.

Estimates[16] show that convective terms in the momentum balance equation (16) are typically negligible compared with the stresses, so that in what follows we take:

$$\nabla\cdot\mathbf{P}^s + \mathbf{n}\cdot(\mathbf{P}^+ - \mathbf{P}^-) = 0, \tag{21}$$

which is simply the classical balance of forces acting on an element of the interface.

The main element where the dividing surface and the continuum-limit-based approaches diverge concerns the parameters characterizing thermodynamics of the interface. In the dividing surface approach, stripped for simplicity to the case of a one-component medium, one deals with 'excess' quantities and as a result has[20] $\rho^s = 0$. Then, the only parameter left to characterize the state of the interface is its temperature[20] T^s, and the only way to arrive at something nontrivial is then to assume that the temperature is discontinuous across the interface and that T^s associated with the massless interface differs from the bulk temperatures T^+ and T^- evaluated at the interface. Should one set $T^+ = T^- = T^s$, the model simply collapses into the Stefan model.

By contrast, in the continuum-limit-based approach we use here, the "interface" is simply an interfacial layer whose thickness is neglected. Then, the surface density is essentially an integral of the density distribution across this layer as opposed to being an integral of the "excess" quantity. Thus, from a thermodynamic viewpoint, the interface can be treated conceptually like a compressible bulk phase and, even in the simplest case of a one-component medium, does not require an assumption that the temperature is discontinuous across the interface for the results to be nontrivial.

We consider the interface to be thermodynamically a two-parameter system, that is, assume it to behave as a pure, simple-compressible substance, whose state is characterized by its temperature T^s and the surface density ρ^s. Then, our interface, not being massless, could, in principle, have a temperature differing from the temperatures of the adjacent bulk phases—and for the clarity of exposition T^s will be kept in the derivation for a short while—but, aiming at the simplest possible model, we will soon set $T^+ = T^- = T^s \equiv T$.

Thus, assuming that the surface phase is a two-parameter thermodynamic system, we can use

$$dU_v^s = T^s\, dS_v^s + \Psi^s\, d\rho^s,$$

where T^s is the temperature of the surface phase to be linked to T^+ and T^- later, S_v^s is its entropy, and Ψ^s is the chemical potential. The subscript v above means, as already clear from Eq. (18), that the quantity refers to the interface contained in a unit volume. In a direct analogy with a two-parametric thermodynamic system in 3D, we define the chemical potential by

$$U_v^s = \rho^s \Psi^s + T^s S_v^s + \sigma,$$

where σ is the surface tension of the interface.

The surface tension in the above equation needs a comment. Discussing the structure and parameters of interfaces, Gibbs[17] was keen to point out the difference between the "surface" and the "interfacial" tension depending on whether it is the molecular-scale layer only on the liquid side of the liquid–solid divide or on both sides that contributes to it. In our consideration, the solid will be treated as rigid and hence, physically, the "interfacial layer" we refer to is a layer on the *liquid* side of the liquid–solid divide where asymmetry of intermolecular forces gives rise to its specific "surface" properties such as the surface tension featuring in the above equation. Notably, as explained by Gibbs,[17] it is the surface tension in this layer that appears in the Young equation, which introduces the notion of the "contact angle" in macroscopic fluid mechanics and which holds if the solid is regarded as rigid.

Now, Eq. (19) can be written down as

$$\begin{aligned}
&T^s\left[\frac{\partial S_v^s}{\partial t} + \nabla\cdot(\mathbf{v}^s S_v^s)\right] + \Psi^s\left[\frac{\partial \rho^s}{\partial t} + \nabla\cdot(\rho^s \mathbf{v}^s)\right] + \sigma\nabla\cdot\mathbf{v}^s \\
&+U_v^+(\mathbf{u}^+ - \mathbf{v}^s)\cdot\mathbf{n} - U_v^-(\mathbf{u}^- - \mathbf{v}^s)\cdot\mathbf{n} \\
&+\frac{1}{2}\rho^+(\mathbf{u}^+ - \mathbf{v}^s)^2(\mathbf{u}^+ - \mathbf{v}^s)\cdot\mathbf{n} - \frac{1}{2}\rho^-(\mathbf{u}^- - \mathbf{v}^s)^2(\mathbf{u}^- - \mathbf{v}^s)\cdot\mathbf{n} \\
&-\mathbf{P}^s : \nabla\mathbf{v}^s - \mathbf{n}\cdot\mathbf{P}^+\cdot(\mathbf{u}^+ - \mathbf{v}^s) + \mathbf{n}\cdot\mathbf{P}^-\cdot(\mathbf{u}^- - \mathbf{v}^s) \\
&+(\mathbf{q}^+ - \mathbf{q}^-)\cdot\mathbf{n} + \nabla\cdot\mathbf{q}^s = 0. \qquad (22)
\end{aligned}$$

Introducing the free energy per unit mass in the bulk phases $F^\pm$ via

$$U_v^\pm = \rho^\pm F^\pm + T^\pm S_v^\pm$$

and using

$$\nabla\cdot\mathbf{q}^s = T^s\nabla\cdot\left(\frac{\mathbf{q}^s}{T^s}\right) + \frac{1}{T^s}\mathbf{q}^s\cdot\nabla T^s,$$

together with the surface mass balance Eq. (15) and the following identity:

$$\begin{aligned}
&-\mathbf{n}\cdot\mathbf{P}^+\cdot(\mathbf{u}^+ - \mathbf{v}^s) + \mathbf{n}\cdot\mathbf{P}^-\cdot(\mathbf{u}^- - \mathbf{v}^s) \\
&= -\frac{1}{\rho^+}\mathbf{n}\cdot\mathbf{P}^+\cdot\mathbf{n} + \frac{1}{\rho^-}\mathbf{n}\cdot\mathbf{P}^-\cdot\mathbf{n} - \frac{1}{2}\mathbf{n}\cdot(\mathbf{P}^+ + \mathbf{P}^-) \\
&\cdot(\mathbf{u}_{||}^+ - \mathbf{u}_{||}^-) + \mathbf{n}\cdot(\mathbf{P}^+ - \mathbf{P}^-)\cdot\left[\mathbf{v}_{||}^s - \frac{1}{2}\left(\mathbf{u}_{||}^+ + \mathbf{u}_{||}^-\right)\right],
\end{aligned}$$

we can write down (22) as

$$\begin{aligned}
&T^s\left[\frac{\partial S_v^s}{\partial t} + \nabla\cdot\left(\mathbf{v}^s S_v^s + \frac{\mathbf{q}^s}{T^s}\right)\right] - \Psi^s\rho^+(\mathbf{u}^+ - \mathbf{v}^s)\cdot\mathbf{n} + \Psi^s\rho^-(\mathbf{u}^- - \mathbf{v}^s)\cdot\mathbf{n} \\
&+(\rho^+F^+ + T^+S_v^+)(\mathbf{u}^+ - \mathbf{v}^s)\cdot\mathbf{n} - (\rho^-F^- + T^-S_v^-)(\mathbf{u}^- - \mathbf{v}^s)\cdot\mathbf{n} \\
&+\frac{1}{2}\rho^+(\mathbf{u}^+ - \mathbf{v}^s)^2(\mathbf{u}^+ - \mathbf{v}^s)\cdot\mathbf{n} - \frac{1}{2}\rho^-(\mathbf{u}^- - \mathbf{v}^s)^2(\mathbf{u}^- - \mathbf{v}^s)\cdot\mathbf{n} \\
&-\mathbf{P}^s : \nabla\mathbf{v}^s + \sigma\nabla\cdot\mathbf{v}^s - \frac{1}{\rho^+}\mathbf{n}\cdot\mathbf{P}^+\cdot\mathbf{n} + \frac{1}{\rho^-}\mathbf{n}\cdot\mathbf{P}^-\cdot\mathbf{n} \\
&-\frac{1}{2}\mathbf{n}\cdot(\mathbf{P}^+ + \mathbf{P}^-)\cdot(\mathbf{u}_{||}^+ - \mathbf{u}_{||}^-) + \mathbf{n}\cdot(\mathbf{P}^+ - \mathbf{P}^-) \\
&\cdot\left[\mathbf{v}_{||}^s - \frac{1}{2}(\mathbf{u}_{||}^+ + \mathbf{u}_{||}^-)\right] + (\mathbf{q}^+ - \mathbf{q}^-)\cdot\mathbf{n} + \frac{1}{T^s}\mathbf{q}^s\cdot\nabla T^s = 0.
\end{aligned}$$

Given that

$$-\mathbf{P}^s : \nabla\mathbf{v}^s + \sigma\nabla\cdot\mathbf{v}^s = -\frac{1}{2}[\mathbf{P}^s - \sigma(\mathbf{I} - \mathbf{nn})] : \left[\nabla\mathbf{v}^s + (\nabla\mathbf{v}^s)^*\right]$$

and now assuming for simplicity that temperature is continuous across the interface,

$$T^+ = T^- = T^s \equiv T, \qquad (23)$$

we arrive at the entropy balance equation in its final form:

$$\begin{aligned}
&\frac{\partial S_v^s}{\partial t} + \nabla\cdot\left(\mathbf{v}^s S_v^s + \frac{\mathbf{q}^s}{T^s}\right) + S_v^+(\mathbf{u}^+ - \mathbf{v}^s)\cdot\mathbf{n} \\
&- S_v^-(\mathbf{u}^- - \mathbf{v}^s)\cdot\mathbf{n} + \left(\frac{\mathbf{q}^+}{T} - \frac{\mathbf{q}^-}{T}\right)\cdot\mathbf{n} \\
&+\frac{\rho^+(\mathbf{u}^+ - \mathbf{v}^s)^2(\mathbf{u}^+ - \mathbf{v}^s)\cdot\mathbf{n}}{2T} - \frac{\rho^-(\mathbf{u}^- - \mathbf{v}^s)^2(\mathbf{u}^- - \mathbf{v}^s)\cdot\mathbf{n}}{2T} \\
&= \frac{1}{T}\left(\Psi^s - F^+ + \frac{1}{\rho^+}\mathbf{n}\cdot\mathbf{P}^+\cdot\mathbf{n}\right)\rho^+(\mathbf{u}^+ - \mathbf{v}^s)\cdot\mathbf{n} \\
&-\frac{1}{T}\left(\Psi^s - F^- + \frac{1}{\rho^-}\mathbf{n}\cdot\mathbf{P}^-\cdot\mathbf{n}\right)\rho^-(\mathbf{u}^- - \mathbf{v}^s)\cdot\mathbf{n} \\
&+\frac{1}{2T}\mathbf{n}\cdot(\mathbf{P}^+ + \mathbf{P}^-)\cdot\left(\mathbf{u}_{||}^+ - \mathbf{u}_{||}^-\right) \\
&-\frac{1}{T}\mathbf{n}\cdot(\mathbf{P}^+ - \mathbf{P}^-)\cdot\left[\mathbf{v}_{||}^s - \frac{1}{2}\left(\mathbf{u}_{||}^+ + \mathbf{u}_{||}^-\right)\right] \\
&+\frac{1}{2T}[\mathbf{P}^s - \sigma(\mathbf{I} - \mathbf{nn})] : \left[\nabla\mathbf{v}^s + (\nabla\mathbf{v}^s)^*\right] - \frac{1}{T^2}\mathbf{q}^s\cdot\nabla T. \qquad (24)
\end{aligned}$$

The right-hand side of this equation is the entropy production. In order to ensure that it is positive, we will follow Onsager's formalism and consider the terms on the right-hand side of Eq. (24) to be products of thermodynamic fluxes and forces, assuming the former to be proportionate to the latter. For simplicity, we will neglect all cross-effects and regard each flux to be proportional only to its own thermodynamic force. An extension to a general case is trivial and will not be considered here.

For the last term, we have

$$\mathbf{q}^s = -\kappa^s \nabla T,$$

which is the Fourier law for the surface phase.

The penultimate term in Eq. (24) yields

$$\mathbf{P}^s - \sigma(\mathbf{I} - \mathbf{nn}) = \mu^s \left[\nabla \mathbf{v}^s + (\nabla \mathbf{v}^s)^*\right],$$

where we assumed isotropy of the surface phase thus ending up with one scalar coefficient of proportionality μ^s, which plays the role of viscosity of the surface phase with respect to shear in the tangential plane. Estimates[16] show that the role of surface viscosity is always negligible compared with the surface tension, so that we may regard the surface phase as ideal, that is, use

$$\mathbf{P}^s = \sigma(\mathbf{I} - \mathbf{nn}). \tag{25}$$

Then, using also that the liquid in the bulk is Newtonian, that is,

$$\mathbf{P}^+ = -p^+ \mathbf{I} + \mu^+ \left[\nabla \mathbf{u}^+ + (\nabla \mathbf{u}^+)^*\right], \tag{26}$$

we can now write down the momentum balance Eq. (21) as

$$\mathbf{n} \cdot \mathbf{P}^- = -p^+ \mathbf{n} + \mu^+ \mathbf{n} \cdot \left[\nabla \mathbf{u}^+ + (\nabla \mathbf{u}^+)^*\right] - \sigma \mathbf{n} \nabla \cdot \mathbf{n} + \nabla \sigma. \tag{27}$$

So far, our equations involved both $\mathbf{u}^-$ and $\mathbf{P}^-$, both evaluated on the solid side of the interface. Should we wish to continue developing a model where dynamics of the solid phase is described, we would need to bring in the solid mechanics, constitutive relationships for the solid phase as well as modification of the heat conduction equation. At this point, we make a simplifying assumption and from now on regard the solid formed by the solidified liquid as rigid. Then, $\mathbf{u}^-$ must be prescribed (e.g., for the process sketched in Fig. 1 $\mathbf{u}^- \equiv 0$) and Eq. (27) will be used in what follows to eliminate $\mathbf{P}^-$.

Using Eq. (27) to eliminate $\mathbf{P}^-$ and considering the terms in Eq. (24) involving parallel components of velocities as products of thermodynamic fluxes and forces, we obtain

$$\mathbf{v}^s_{||} - \frac{1}{2}\left(\mathbf{u}^+_{||} + \mathbf{u}^-_{||}\right) = \alpha \nabla \sigma,$$
$$\mu^+ \mathbf{n} \cdot \left[\nabla \mathbf{u}^+ + (\nabla \mathbf{u}^+)^*\right] \cdot (\mathbf{I} - \mathbf{nn}) + \frac{1}{2}\nabla \sigma = \beta\left(\mathbf{u}^+_{||} - \mathbf{u}^-_{||}\right).$$

These two equations are exactly the same as in Ref. 16 (see also Appendix in Ref. 13) with the coefficients of proportionality α and β characterizing the response of the surface phase to the surface tension gradient and an external torque, respectively.

Finally, we come to the first two terms on the right-hand side of Eq. (24), which involve mass exchanges between the surface and bulk phases. The bulk liquid is assumed to be incompressible, and therefore, as is well known,[26] its thermodynamic state is characterized only by its temperature. Then, evaluating its free energy at the interface, we have

$$F^+ = F^+(T), \tag{28}$$

as the temperature is continuous across the interface. The solid is regarded as rigid and for it, for simplicity, we assume

$$F^- = F^-(T). \tag{29}$$

We will return to this assumption in Sec. VII, and here only point out that unlike the liquid, where (28) is a consequence of the assumption of incompressibility, Eq. (29) does not necessarily follow from the assumption that the solid is regarded as rigid. It is an assumption in its own right since the free energy of a solid can depend also on the parameters characterizing its microstructure.

For the surface phase, we can take $\Psi^s = \Psi^s(\rho^s, T)$ and, after using Eqs. (26) and (27) in the first two terms of Eq. (24) and, as before, making the thermodynamic fluxes proportional to the corresponding forces, obtain

$$\rho^+(\mathbf{u}^+ - \mathbf{v}^s) \cdot \mathbf{n} = k_{\rho+}\left(\Psi^s(\rho^s, T) - F^+(T) - \frac{p^+}{\rho^+} + \frac{\mu^+ \mathbf{n} \cdot \left[\nabla \mathbf{u}^+ + (\nabla \mathbf{u}^+)^*\right] \cdot \mathbf{n}}{\rho^+}\right), \tag{30}$$

$$\rho^-(\mathbf{u}^- - \mathbf{v}^s) \cdot \mathbf{n} = -k_{\rho-}\left(\Psi^s(\rho^s, T) - F^-(T) - \frac{p^+}{\rho^-} + \frac{\mu^+ \mathbf{n} \cdot \left[\nabla \mathbf{u}^+ + (\nabla \mathbf{u}^+)^*\right] \cdot \mathbf{n}}{\rho^-} - \frac{\sigma \nabla \cdot \mathbf{n}}{\rho^-}\right). \tag{31}$$

Estimates show that the last term in brackets on the right-hand side of Eq. (30) and the last two terms in Eq. (31) may be neglected. Indeed, assuming that characteristic velocity, viscosity, length scale, and the surface tension are $\sim$1 m/s, $\sim$1 mPa s, $\sim 10^{-2}$ cm, and $\sim 10^2$ mN/m, we have that for $p^+ \sim 1$ atm, the contribution of the viscous stresses and capillary pressure is less than 0.01 of p^+.

Thus, in the brackets on the right-hand side of Eqs. (30) and (31) we are left with what is in essence the difference of chemical potentials. Instead of specifying Ψ^s and $F^\pm$ explicitly, it is more convenient to introduce two equilibrium surface densities $\rho^s_{\mathrm{eq},\pm}(T, p)$ expressing them in terms of Ψ^s:

$$\Psi^s(\rho^s_{\mathrm{eq},\pm}(T, p^+), T) = F^\pm(T) + \frac{p^+}{\rho^\pm}. \tag{32}$$

Then, if $\rho^s = \rho^s_{\mathrm{eq},+}$ or $\rho^s = \rho^s_{\mathrm{eq},-}$, there is no mass exchange between the surface phase and the corresponding bulk phase. The melting temperature T_m is then defined as

$$\rho^s_{\mathrm{eq},+}(T_m, p^+) = \rho^s_{\mathrm{eq},-}(T_m, p^+). \tag{33}$$

We can also introduce the relaxation times $\tau_\pm$ corresponding to equilibration of the surface phase with the corresponding bulk phase:

$$\tau_\pm(T, p) = \frac{1}{k_{\rho\pm}\dfrac{\partial \Psi^s}{\partial \rho^s}(\rho^s_{\mathrm{eq},\pm}(T, p^+), T)}$$

so that (30), (31) can now approximately, that is, to leading order in the differences $\rho^s - \rho^s_{\mathrm{eq},\pm}$, be written down as

$$\rho^\pm(\mathbf{u}^\pm - \mathbf{v}^s) \cdot \mathbf{n} = \pm \frac{\rho^s - \rho^s_{\mathrm{eq},\pm}}{\tau_\pm}. \tag{34}$$

Finally, we consider the energy balance of the surface phase (19) where now expressions (25), (26), and (27) are used for $\mathbf{P}^s$, $\mathbf{P}^+$ and $\mathbf{n} \cdot \mathbf{P}^-$:

$$\frac{\partial U_v^s}{\partial t}+\nabla\cdot(\mathbf{v}^s U_v^s)+\left(U^+ +\frac{p^+}{\rho^+}\right)\rho^+(\mathbf{u}^+-\mathbf{v}^s)\cdot\mathbf{n}$$
$$-\left(U^- +\frac{p^+}{\rho^-}\right)\rho^-(\mathbf{u}^--\mathbf{v}^s)\cdot\mathbf{n}$$
$$+\frac{1}{2}\rho^+(\mathbf{u}^+-\mathbf{v}^s)^2(\mathbf{u}^+-\mathbf{v}^s)\cdot\mathbf{n}-\frac{1}{2}\rho^-(\mathbf{u}^--\mathbf{v}^s)^2(\mathbf{u}^--\mathbf{v}^s)\cdot\mathbf{n}$$
$$-\mu^+\mathbf{n}\cdot\left[\nabla\mathbf{u}^+ +(\nabla\mathbf{u}^+)^*\right]\cdot(\mathbf{u}^+-\mathbf{u}^-)$$
$$+(\nabla\sigma-\sigma\mathbf{n}\nabla\cdot\mathbf{n})\cdot(\mathbf{u}^--\mathbf{v}^s)$$
$$-\sigma\nabla\cdot\mathbf{v}^s+(\mathbf{q}^+-\mathbf{q}^-)\cdot\mathbf{n}+\nabla\cdot\mathbf{q}^s=0,$$

Straightforward estimates show that the dominant terms in this equation are those with the heat fluxes and convective energy fluxes from the bulk phases, so that

$$\left(U^+ +\frac{p^+}{\rho^+}\right)\rho^+(\mathbf{u}^+-\mathbf{v}^s)\cdot\mathbf{n}-\left(U^- +\frac{p^+}{\rho^-}\right)\rho^-(\mathbf{u}^--\mathbf{v}^s)\cdot\mathbf{n}$$
$$+(\mathbf{q}^+-\mathbf{q}^-)\cdot\mathbf{n}=0. \tag{35}$$

In this equation, one can use $U^\pm=c^\pm T+U_0^\pm$ and $\mathbf{q}^\pm=-\kappa^\pm\nabla T^\pm$, where, as before, $c^\pm$ are specific heats and $\kappa^\pm$ are thermal conductivities of the bulk phases.

Now, we can write down the boundary conditions, which, as shown below, generalize both the Stefan model of Sec. II and the model resolving the moving contact-line problem:[13]

$$\frac{\partial f}{\partial t}+\mathbf{v}^s\cdot\nabla f=0, \tag{36}$$

$$\frac{\partial\rho^s}{\partial t}+\nabla\cdot(\rho^s\mathbf{v}^s)=-\rho^+(\mathbf{u}^+-\mathbf{v}^s)\cdot\mathbf{n}+\rho^-(\mathbf{u}^--\mathbf{v}^s)\cdot\mathbf{n}, \tag{37}$$

$$\rho^\pm(\mathbf{u}^\pm-\mathbf{v}^s)\cdot\mathbf{n}=\pm\frac{\rho^s-\rho^s_{\mathrm{eq},\pm}(T,p^+)}{\tau_\pm(T,p^+)}, \tag{38}$$

$$\mathbf{v}^s_\parallel=\frac{1}{2}\left(\mathbf{u}^+_\parallel+\mathbf{u}^-_\parallel\right)+\alpha\nabla\sigma(\rho^s,T), \tag{39}$$

$$\mu^+\mathbf{n}\cdot\left[\nabla\mathbf{u}^+ +(\nabla\mathbf{u}^+)^*\right]\cdot(\mathbf{I}-\mathbf{nn})+\frac{1}{2}\nabla\sigma(\rho^s,T)=\beta\left(\mathbf{u}^+_\parallel-\mathbf{u}^-_\parallel\right), \tag{40}$$

$$(\kappa^+\nabla T^+-\kappa^-\nabla T^-)\cdot\mathbf{n}=\left(c^+T+\frac{p^+}{\rho^+}+U_0^+\right)\rho^+(\mathbf{u}^+-\mathbf{v}^s)\cdot\mathbf{n}$$
$$-\left(c^-T+\frac{p^+}{\rho^-}+U_0^-\right)\rho^-(\mathbf{u}^--\mathbf{v}^s)\cdot\mathbf{n}, \tag{41}$$

$$T^+=T^-=T, \tag{42}$$

where Eq. (41) is Eq. (35) rearranged as described above.

This set of boundary conditions is not yet ready for practical use as it needs to be closed by specifying the functions $\rho^s_{\mathrm{eq},\pm}(T,p^+)$, $\tau_\pm(T,p^+)$, and $\sigma(\rho^s,T)$. It should be noted that an assumption of all these functions being constants is not an option even as the crudest approximation. At the very least, one has to specify the dependence of $\rho^s_{\mathrm{eq},\pm}$ on T as well as the dependence of σ on ρ^s and, for essentially non-isothermal processes, on T: the former is key to the phase transition phenomena while the latter is crucial for dynamic wetting.

In what follows, for brevity, we will use the notation:

$$H^\pm(T,p^+)=c^\pm T+\frac{p^+}{\rho^\pm_\pm}+U_0^\pm.$$

Note that boundary conditions (36)–(42) include no mechanical characteristics of the solid, only its velocity $\mathbf{u}^-$, which is assumed to be specified.

D. Closure

All material properties of the phases associated with their interaction are now accumulated in four functions $\rho^s_{\mathrm{eq},\pm}(T,p^+)$ and $\tau_\pm(T,p^+)$, while the surface equation of state0 required to describe the dynamics of the surface phase is to be specified as $\sigma=\sigma(\rho^s,T)$. Ultimately, all these function are to be determined experimentally as they will be different, certainly quantitatively, for different systems. However, some qualitative features of these functions can be inferred from general considerations so that, for the time being, simple relationships can be proposed to close the system of boundary conditions (36)–(42) and hence make them usable.

For the densities $\rho^s_{\mathrm{eq},\pm}$ as functions of T we know that they satisfy (33), that is, coincide at one point, thus defining the melting temperature T_m. The slopes of $\rho^s_{\mathrm{eq},\pm}$ as functions of T at this point can be inferred from the following consideration. If for a system in equilibrium, where, according to Eq. (33), $\rho^s_{\mathrm{eq},+}(T_m,p^+)=\rho^s=\rho^s_{\mathrm{eq},-}(T_m,p^+)$, we have a temperature fluctuation such that $T<T_m$, then, for the system to return to equilibrium, this should trigger solidification of the liquid; that is, we should have $\rho^s_{\mathrm{eq},-}<\rho^s<\rho^s_{\mathrm{eq},+}$ and hence the solidification process, while for $T>T_m$ this should trigger melting of the solid; that is, we should have $\rho^s_{\mathrm{eq},+}<\rho^s<\rho^s_{\mathrm{eq},-}$. Thus, at equilibrium we have

$$\frac{\partial\rho^s_{\mathrm{eq},+}}{\partial T}<0,\quad \frac{\partial\rho^s_{\mathrm{eq},-}}{\partial T}>0,$$

which corresponds to the phase diagram in the (T,ρ^s)-plane sketched in Fig. 2. Then, in the vicinity of the melting temperature we can assume

$$\rho^s_{\mathrm{eq},\pm}=\rho^s_*[1\mp a_\pm(T-T_m)], \tag{43}$$

where ρ^s_*, $a_\pm>0$ and T_m are functions of p^+. In practice, this dependence on p^+ can often be neglected as the variation of p^+ in processes of interest is typically relatively small.

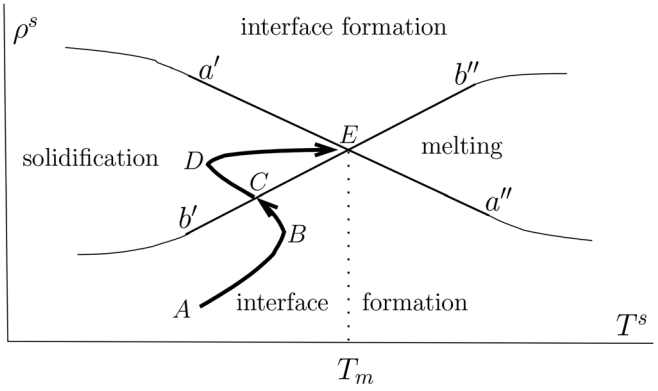

FIG. 2. The phase diagram in the (T,ρ^s) plane with p^+ fixed. a'-a'': $\rho^s=\rho^s_{\mathrm{eq},+}(T,p^+)$; b'-b'': $\rho^s=\rho^s_{\mathrm{eq},-}(T,p^+)$. The path $A\to B\to C\to D\to E$ corresponds to a typical process for an initially rarefied (liquid/gas) interface impulsively brought in contact with a solid: $A\to C$: interface formation where the temperature rises above the one the interface had immediately after contact ($A\to B$) and then decreases ($B\to C$); C: the onset of solidification; $C\to D$: transitional/unbalanced solidification; $D\to E$: balanced solidification; E: equilibrium.

For $\tau_\pm(T,p^+)$, we can only plausibly assume that τ_+, which characterizes interaction of the surface phase with the liquid, decreases with T, while τ_- responsible for solidification increases as T goes up. In the simplest case, assuming that the temperature dependence near T_m is linear, we then have

$$\tau_\pm = \tau_{*,\pm}[1 \mp b_\pm(T - T_m)], \tag{44}$$

where again $\tau_{*,\pm}$ and $b_\pm > 0$ depend on p^+. This dependence is to be specified or, as an initial approximation, neglected.

Finally, for a given temperature, the surface tension is associated with rarefication or compression of the fluid in the surface phase due to asymmetry of intermolecular forces from the bulk phases. In the liquid–gas interfacial layer, the liquid is rarefied while in contact with a solid it can be rarefied or compressed depending on the wettability of the solid with respect to this liquid. Thus, in the simplest case this can be modeled as a linear dependence:

$$\sigma = \gamma(T)\left[\rho_0^s(T) - \rho^s\right]. \tag{45}$$

This is the same dependence on ρ^s as the one successfully used, for example, in Refs. 13 and 27–30 with the only difference that now coefficients γ and ρ_0^s are functions of T. Physically, γ, having the dimension of the speed squared, reflects compressibility of the liquid, while ρ_0^s is a reference surface density corresponding to the interfacial layer in the absence of asymmetry of intermolecular forces. One can also see ρ_0^s as the surface density in the liquid–solid interface where the solid has neutral wettability corresponding to the contact angle formed by the free surface with it equal to 90°. From the physical meaning of these coefficients, one can infer that $\gamma(T)$ is an increasing and $\rho_0^s(T)$ is a decreasing function of T and, for simplicity, assume

$$\gamma(T) = \gamma(T_m)[1 + \gamma_1(T - T_m)],$$
$$\rho_0^s(T) = \rho_0^s(T_m)[1 - q_1(T - T_m)],$$

where the coefficients γ_1 and q_1 in the first term of the power series expansion of γ and ρ_0^s about T_m are positive constants.

IV. STEFAN PROBLEM AND DYNAMIC WETTING MODEL AS LIMITING CASES

In order to model such flows as the spreading and solidification of molten drops on cold substrates and the arrest of the contact-line motion,[5] both solidification and dynamic wetting should be described in the same conceptual and mathematical framework. The first step in showing that the framework developed above is the required one is to show that boundary conditions (36)–(42) have both the Stefan problem outlined in Sec. II and the part related to the substrate of the model solving the moving contact-line problem in an isothermal case[13] as their limiting cases.

A. Reduction to the Stefan problem

Consider boundary conditions (36)–(42) in the limit $\tau_+ \sim \tau_- \to 0$, $\alpha \to 0$, $\beta \to \infty$, which for a particular problem will be cast in terms of the appropriate dimensionless similarity parameters. Then, first, condition (53) will turn into Eq. (5), that is,

$$\rho^+(\mathbf{u}^+ - \mathbf{v}^s)\cdot\mathbf{n} = \rho^-(\mathbf{u}^- - \mathbf{v}^s)\cdot\mathbf{n}. \tag{46}$$

Conditions (39), (40) in the limit $\alpha \to 0$, $\beta \to \infty$ yield (6), that is,

$$\mathbf{u}_{||}^+ = \mathbf{u}_{||}^- = \mathbf{v}_{||}^s. \tag{47}$$

Taking the limit $\tau_\pm \to 0$ in Eq. (38) and eliminating ρ^s, we obtain $\rho^s_{\mathrm{eq},+}(T,p^+) = \rho^s_{\mathrm{eq},-}(T,p^+)$ or, invoking the definition (33) and bringing in Eq. (42), end up with

$$T^+ = T^- = T_m, \tag{48}$$

that is, condition (7) of the Stefan problem.

Finally, introducing the notation

$$H_L = H^+(T_m,p^+) - H^-(T_m,p^+)$$
$$= (c^+ - c^-)T_m + p^+\left(\frac{1}{\rho^+} - \frac{1}{\rho^-}\right) + U_0^+ - U_0^-$$

for the latent heat of fusion and using Eq. (46) once again, we can write down (41) in the form of the Stefan condition (8), that is,

$$(\kappa^+\nabla T^+ - \kappa^-\nabla T^-)\cdot\mathbf{n} = H_L\rho^+(\mathbf{u}^+ - \mathbf{v}^s)\cdot\mathbf{n}. \tag{49}$$

Thus, the Stefan problem appears, thermally, in the limit of the characteristic time scales of the process under consideration large compared with the relaxation times $\tau_\pm$ and, dynamically, with the velocity difference across the interface neglected.

B. Reduction to the moving contact-line problem

As shown in Ref. 13, the only mathematical model to date capable of describing both spontaneous and forced dynamic wetting is the model of this phenomenon as a process of interface disappearance and formation, a process where the liquid–gas interface disappears into the contact line and a fresh liquid–solid interface forms. As a matter of fact, the very term "dynamic wetting" refers to the appearance of a newly wet solid surface, that is, the formation of a fresh liquid-solid interface. The corresponding model, originated in Ref. 27, came to be known as the interface formation model (IFM), and the first 15 years of its development and application are summarized in Ref. 16. What we need to show now is that the model developed in Sec. III generalizes the part of the IFM dealing with the solid substrate.

If we (i) formally take $\tau_- \to \infty$, that is, consider the substrate to be of a different material than the liquid and not reacting with the latter, and (ii) for simplicity neglect the dependence of the model's parameters on temperature, thus assuming variation of the latter to be small, then we can immediately see that Eq. (38) for the upper sign, Eqs. (40) and (38) for the lower sign, Eqs. (53), (39), and (45) turn, respectively, into

$$(\mathbf{u}^- - \mathbf{v}^s)\cdot\mathbf{n} = 0, \tag{50}$$

$$\mu^+\mathbf{n}\cdot\left[\nabla\mathbf{u}^+ + (\nabla\mathbf{u}^+)^*\right]\cdot(\mathbf{I} - \mathbf{nn}) + \frac{1}{2}\nabla\sigma = \beta\left(\mathbf{u}_{||}^+ - \mathbf{u}_{||}^-\right), \tag{51}$$

$$\rho^+(\mathbf{u}^+ - \mathbf{v}^s)\cdot\mathbf{n} = \frac{\rho^s - \rho^s_{\mathrm{eq},+}}{\tau_+}, \tag{52}$$

$$\frac{\partial\rho^s}{\partial t} + \nabla\cdot(\rho^s\mathbf{v}^s) = -\frac{\rho^s - \rho^s_{\mathrm{eq},+}}{\tau_+}, \tag{53}$$

$$\mathbf{v}_{||}^s = \frac{1}{2}\left(\mathbf{u}_{||}^+ + \mathbf{u}_{||}^-\right) + \alpha\nabla\sigma, \tag{54}$$

$$\sigma = \gamma\left(\rho_0^s - \rho^s\right), \tag{55}$$

that is boundary conditions (A8)–(A13) of the interface formation model listed in Appendix of Ref. 13 where the simplest variant of the

IFM is summarized. Once the dependence of parameters on temperature is taken into account, we end up with the moving contact-line problem with thermal effects.

V. SOLIDIFICATION FRONT AND ITS EDGE

A. Phase transition as an interface formation process

The key element of the model (36)–(42), Eq. (45) is that, besides an external (shared with the bulk) parameter T, the state of the surface phase is determined also by an internal parameter ρ^s, and it is the value of the latter that determines whether the surface phase is in equilibrium or whether an equilibrium is at all possible at a given temperature. In an out-of-equilibrium state, both ρ^s and T evolve trying to equilibrate the surface phase with both bulk phases, and the evolution of T shared by the surface and bulk phases causes thermal effects in the bulk.

If $T < T_m$, then $\rho^s_{\mathrm{eq},+} > \rho^s_{\mathrm{eq},-}$ and for

$$\rho^s_{\mathrm{eq},-}(T,p^+) < \rho^s < \rho^s_{\mathrm{eq},+}(T,p^+), \tag{56}$$

according to Eq. (38), we have a mass flux from the bulk liquid into the surface phase trying to drive ρ^s toward $\rho^s_{\mathrm{eq},+}$ and hence the surface phase toward its equilibrium with the liquid. At the same time, we also have a mass flux from the surface phase into the solid; that is, the solid is trying to drive ρ^s toward $\rho^s_{\mathrm{eq},-}$ and away from $\rho^s_{\mathrm{eq},+}$, so that the interface is being driven toward its equilibrium with the solid and away from its equilibrium with the liquid. Thus, considering this dual process from the viewpoint of either bulk phase, one can say that the surface phase is forming with respect to it while the other bulk phase is trying to drive the process in the opposite direction. As a result of these competing processes, there is a net mass flux from one bulk phase into the other, in this case from the liquid into the solid, and we have a phase transition, in this case solidification.

Similarly, the situation where $T > T_m$ and

$$\rho^s_{\mathrm{eq},+}(T,p^+) < \rho^s < \rho^s_{\mathrm{eq},-}(T,p^+), \tag{57}$$

corresponds to melting with the net mass flux across the interface going the other way. The case where the fluxes into and out of the surface phase are equal can be referred to as balanced/pure phase transition as opposed to unbalanced/transitional phase transition where the processes of equilibration of the surface phase with respect to the bulk phases occur at different rates. The Stefan regime is then simply the limiting case of the balanced phase transition where $T \to T_m$.

Inequalities (56) and (57) correspond to the regions in the phase diagram of Fig. 2 labeled "solidification" and "melting," respectively. In addition to these situations, the parameters of the surface phase T and ρ^s can be such that $\rho^s < \rho^s_{\mathrm{eq},\pm}$, and hence, the mass fluxes from *both* bulk phases are into the surface phase. This situation can be referred to as pure interface formation with no phase transition (Fig. 2). Physically, this is the case, for example, in dynamic wetting of an inert substrate[13] where $\tau_- = \infty$, and hence, the flux from the solid phase is zero with the line $\rho^s = \rho^s_{\mathrm{eq},-}$ in Fig. 2 irrelevant and the interface formation occurring solely due to the mass exchange with the liquid phase.

B. The edge of solidification front

Now, we can specify what the leading edge of the solidification front is. In the situation where the liquid spreads over and solidifies on a substrate of a different material inert with respect to it, the answer is simple: the leading edge of the solidification front is where the solidified liquid as a bulk phase appears. In the context of the drop spreading (Fig. 1), the out-of-equilibrium liquid–solid interface left behind the moving contact line has to equilibrate only with respect to the liquid phase as there is no mass exchange between the surface phase and the (inert) substrate (see Sec. IV B). Once ρ^s, as it relaxes toward $\rho^s_{\mathrm{eq},+}$, rises above $\rho^s_{\mathrm{eq},-}$, solidification of the liquid begins. Thus, the leading edge of the solidification front in Fig. 1(c) is the point where, for $T < T_m$, one has

$$\rho^s = \rho^s_{\mathrm{eq},-}(T,p^+). \tag{58}$$

If the substrate is made of the same material as the liquid, that is, solidified liquid is present from the start albeit at a different temperature than the melt, the situation is slightly more intricate. Dynamic wetting as such occurs in its usual way, that is, the moving contact line leaves behind an out-of-equilibrium freshly created liquid–solid interface, but now equilibration of the latter involves the influx from both bulk phases as it is out of equilibrium and can exchange mass with both of them, $\rho^s < \rho^s_{\mathrm{eq},\pm}$. This inequality is due to the fact that the liquid–solid interface is created out of the liquid–gas one after the latter passes through the contact line ("rolling motion")[16] and the surface density in the liquid–gas interface is considerably lower than that in the liquid–solid interface.[16,31]

The situation is particularly transparent in the case of an impacting drop. Following the impact, the drop goes into the so-called geometric (or kinematic) wetting regime [Fig. 1(b)] where the drop deforms, and the radius of its base expands $\propto \sqrt{t}$. This, initially infinite, rate of creation of the liquid–solid area of contact means that initially the interface is essentially the free surface, which now finds itself squeezed between the two bulk phases and has to adjust to its new environment. Thus, one has $\rho^s < \rho^s_{\mathrm{eq},\pm}$, and the liquid–solid interface then takes in mass from both bulk phases, which is pure interface formation (Fig. 2).

Spatially, the freshly created liquid–solid interface is not uniform as different parts of it have been created at different times. Like in the case of isothermal dynamic wetting,[16,27] the surface density increases as one goes away from the moving contact line, and as it reaches $\rho^s_{\mathrm{eq},-}$ for $T < T_m$ and then exceeds this value, the direction of the mass flux between the solid and the surface phase changes: now, it is into the solid, and hence, there appears a net mass flux from the liquid into the solid. Thus, condition (58) corresponds to the point where pure interface formation gives way to solidification. The latter, at first, is in the unbalanced regime as, by continuity, the flux from the surface phase into the solid is yet smaller than from the liquid into the surface phase. As ρ^s increases, the fluxes balance and the process moves toward the Stefan regime. Schematically, this evolution is shown in Fig. 2.

Thus, the edge of the solidification is defined by Eq. (58) irrespective of the material of the substrate. The only difference between the substrate of the same material as the liquid and of a different one is that for the former the interface formation in front of the moving edge involves mass exchange with both bulk phases (which actually means melting of the substrate on the microscopic level) while for the latter the mass exchange is solely with the liquid. Behind the edge, in both cases one has solidification, which, for the substrate of the same material, adds mass to the preexisted solid phase while for the substrate of a different material it produces a new bulk phase.

The question as to what angle the solidification front forms with the substrate has a simple answer. A local asymptotic analysis of the parameter distributions near the edge in the limit $r \to 0$, where r is the distance from the edge, shows that there is no singularity in the heat flux only if the substrate ahead of the edge turns into the solidification front smoothly, that is, the "contact angle" between the solidification front and the preexisting substrate is zero. This is easy to understand given that in this case there is no discontinuity in the boundary conditions across the edge nor is there any angle while, should there be an angle, one would have two adjacent wedge regions and, as is known, the heat fluxes would have had a singularity even if they and the temperatures are assumed to be continuous across the boundaries.

VI. ARREST OF THE CONTACT LINE MOTION

The experiments on a molten drop impacting onto a cold solid substrate show that

(a) the spreading after the impact is "experimentally indistinguishable" from what it is in an isothermal case[5] with the substrate undercooling qualitatively playing no role[8] until
(b) the spreading is arrested[4–8] such that
(c) the higher the substrate undercooling, the smaller the maximum radius of the drop's base and, correspondingly, the higher the contact angle that the drop's surface forms with the substrate.[4,8]

Consider how (a)–(c) could be explained, at this stage qualitatively, in terms of the developed framework.

The first of these features is obvious: the starting point for developing the framework is that dynamic wetting and solidification occur as separate phenomena, which allows for the scheme of the drop impact process sketched in Fig. 1. Then, the initial stages of the process [Figs. 1(b) and 1(c)] from the viewpoint of the free-surface evolution as it is observed experimentally are the same as in the isothermal case, that is, not affected by solidification. As for the undercooling, the temperature obviously influences parameters of the model so that quantitatively the degree of undercooling will have an effect on the spreading but on a qualitative level it is the same as in the isothermal case.

The arrest of the contact line, seen as abrupt from the viewpoint of the preceding spreading, happens over a short but finite time, as can be seen in experiments.[4,8] In terms of the present model, once the edge of the solidification front catches up with the contact line, it cannot move any further. One can say that from the viewpoint of the solidification edge, it is the contact line that arrests its further propagation along the substrate. From this moment onward, condition (58) defining the position and the speed of propagation of a freely moving edge no longer has to be satisfied, and ρ^s at the contact line (i.e., the limit of ρ^s as one approaches the contact line along the solidification front as ρ^s *at* the contact line itself is obviously not defined) will increase, leading to the mass transfer from the surface phase into the solid and consequently resulting in the edge of the solidification front departing from the contact line and climbing up the liquid–gas interface [Fig. 1(e)]. Thus, the moment when the edge catches up with the contact line corresponds to the arrest of the contact line motion; after this, the edge will propagate not along the substrate but up the free surface.

The deceleration of the spreading begins when the edge of the solidification front reaches the surface-tension-relaxation "tail" left behind the moving contact line, similarly to the mechanism of hydrodynamic influence on the dynamic contact angle observed in curtain coating.[32]

Regarding the effect of the substrate undercooling, it is reasonable to expect that the speed of propagation of the solidification edge increases with the substrate undercooling simply given the slope of $\rho^s = \rho^s_{\mathrm{eq}_-}$ in Fig. 2: crudely, the lower the temperature, the shorter the $A \to C$ path. The same follows from the basic continuity argument: with no undercooling the edge simply does not appear, and hence, with very low undercooling it will appear but propagate slowly. Hence, the time to the contact line arrest and the size of the drop's maximum base, being inversely proportional to the speed of the edge propagation, will become smaller as the substrate undercooling increases. The contact angle formed by the solidified drop with the substrate will become correspondingly larger.

Although the details of numerical implementation of the interface formation model have now been fully explained,[30,33] the quantitative modeling of the whole process of the drop impact, spreading and solidification, that is, with phase transition on a free boundary and thermal effects on top of dynamic wetting, is a challenging numerical problem to be addressed in a separate publication.

VII. DISCUSSION

The conceptual framework introduced in Sec. III incorporates liquid–solid phase transitions as well as wetting phenomena with thermal effects into the toolkit of continuum mechanics as standard elements. This allows one to formulate and solve a variety of problems in a regular way. From the mathematical modeling viewpoint, the key difference between the new approach and the currently prevalent one is as follows.

Since Wilson's pioneering formula[34] proposed in 1900 and still in use today in continuum mechanics under the name of "kinetic undercooling,"[35,36] all theories of solidification in physical chemistry are aimed at expressing the velocity at which the solidification front propagates as a function of the temperature at the front, various activation energies, energy of growth, configurational entropy, enthalpy, and other such concepts. From the viewpoint of continuum mechanics, this function is then to be used as a kinematic boundary condition generalizing linear kinetic undercooling.[34,35] A critical analysis from the physical chemist's viewpoint of these theories and the functions they propose can be found in Ref. 37 where another function of the same variety is advocated as an alternative. All this activity resembles the situation that until recently took place in dynamic wetting where for the past fifty years, since the seminal work of Huh and Scriven[15] of 1971, the focus has also been on finding a formula expressing the dynamic contact angle as a function of the contact-line speed and material constants. However, the growing number of discrepancies between what this approach could offer and experimental observations; for example, Refs. 32 and 38 have eventually led to a simple argument, expressible even in a graphical form,[13] showing that the coveted function does not exist in principle and that the contact angle behavior should be an outcome in the solution of a particular problem, different for different problems, rather than a prescribed input in the model used to obtain this solution.

The developed framework for the modeling of solidification presents an alternative to the approach outlined above as in it the velocity of the solidification front is not prescribed neither as a

function of temperature nor in any other way and has to be found as part of the solution of a particular problem. This is illustrated by the curve C–D–E in Fig. 2, which qualitatively summarizes the numerical results for a 1D propagation of the solidification front. As one can see, the same temperature can correspond to different values of ρ^s and hence different speeds of propagation of the solidification front. The same applies to the dynamic contact angle in dynamic wetting processes given that the present work merely extends the interface formation theory[16] to a non-isothermal case where this feature is present; see Fig. 14 in Ref. 30 and a discussion in Ref. 13.

In other words, instead of prescribing the kinematic and geometric features of a process (i.e., the front's velocity and the contact angle) as given functions fundamental to all processes, the developed approach makes them subject to the underlying physical laws describing how chemical potentials of the contacting phases negotiate the velocity of the liquid–solid interface and how the forces acting on the contact line negotiate the appropriate value of the contact angle.

The simplest model of Sec. III already makes it possible to formulate and solve problems. However, there are some experimentally observed features in the solidification dynamics already calling for further development of the model. For example, experiments show that even not too far from the melting temperature both the solidification front itself and its edge propagating across a solid substrate can exhibit rather complex behaviors and structures: the front can be covered with needlelike columnar dendrites, which appear for low undercooling of the substrate, while for higher undercooling these morphologies are not observed,[10] crystalline clouds can organize themselves into circular bands,[10] the edge can emit ligaments[11] to mention but some effects. Therefore, it seems reasonable to examine the simplest model from the viewpoint of identifying the main 'branch points' from which essential generalizations could stem.

The most obvious branch point is the constitutive relations where, for simplicity, we neglected all cross-effects and considered only the direct pairing of thermodynamic forces and fluxes. Once the cross-effects are accounted for, like, for example, in Refs. 20, 22, and 24, the model will be expected to exhibit a host of new features even on a qualitative level.

In the present framework, the solidified liquid is regarded as rigid (undeformable), which is an essential simplification as it completely excludes the dynamics of the solid from consideration thus making the solid boundary just a geometric constraint for the fluid flow. In this regard, one would be interested in describing the complexity of the solidification front morphologies observed experimentally but still without bringing in deformability of the solid and all what comes with it in the continuum mechanics modeling. The key here is in the assumption (29). For an incompressible liquid, the corresponding Eq. (28) is not an assumption; it is a consequence of incompressibility[26] reflecting the fact that, microscopically, the liquid is structureless. Then, once the density is regarded constant, it is only the temperature that determines the liquid's thermodynamic state. By contrast, Eq. (29) is an assumption as it means that the possible dependence of the free energy on the parameters characterizing the structure of the medium on the microscopic level is neglected. Should (29) be generalized, one would end up with $F^- = F^-(T, \chi_1, \ldots)$, where χ_i, $(i = 1, \ldots)$ are parameters describing the microstructure, for example, in crystallographic terms. A wealth of knowledge regarding the functional form of the free energy is accumulated in the phase-field modeling of crystallization,[39,40] which, so far, remains unconnected with macroscopic continuum mechanics. This work offers a framework for this connection to be made. Some or all of the parameters in the free energy should then have their counterparts characterizing the surface phase as the latter should mirror the ordering of the solid into which the material of the surface phase disappears in the solidification process. Here, again the phase-field theory could offer some insight though the coupling of the 2D surface and the bulk solid in terms of continuum mechanics modeling is a nontrivial task. The first step in this direction could, perhaps, be introducing one additional parameter of state only in the surface phase, similar in its type to the order parameter, and keeping (29) intact. This would allow utilizing the 2D variant of the phase-field approach in a relatively straightforward way.

The last branch point to be mentioned here is Eq. (32) where the equilibrium surface densities $\rho^s_{\mathrm{eq},\pm}$ are introduced. This and the subsequent expansion of the deviation of the chemical potential Ψ^s from its equilibrium value allowed us to express the mass exchange between the surface and bulk phases in the form of Eq. (34), that is, via easily interpretable concepts of the equilibrium surface densities $\rho^s_{\mathrm{eq},\pm}$ and the corresponding relaxation times $\tau_\pm$ for both of which the closure relationships could then be plausibly formulated. Departing from these concepts at this point would mean that one will need to operate with an explicit form of $\Psi^s = \Psi^s(\rho^s, T)$ or, to use an analogy with the bulk phase $\Psi^s(\sigma, T)$. Whether or not this nonlinear route is worth pursuing is not clear given that, as the example of the Navier–Stokes equations shows, the linear constitutive relationships typically work very well for the entire parameter range of practical interest.

Finally, it should be noted that the present extension of the original interface formation model[27] to a non-isothermal situation in its dynamic wetting part is applicable only to liquid/*gas*/solid systems. For liquid/liquid/solid systems, the interface formation model to start from is given in Ref. 16, with its precursor published in Ref. 41, but its extension to incorporate non-isothermal effects including phase transitions is a nontrivial task. The main obstacle is that, unlike a gas, a displaced liquid invariably leaves behind a microscopic residual film,[42] even if the solid is non-wettable by it,[43,44] so that the composition of the interface between the advancing liquid and the solid substrate appears to be considerably more complex than the one considered here.

ACKNOWLEDGMENTS

The support of the Engineering and Physical Sciences Research Council (UK) via Programme Grant EP/P031684/1 is gratefully acknowledged.

DATA AVAILABILITY

Data sharing is not applicable to this article as no new data were created or analyzed in this study.

REFERENCES

[1]A. Lores, N. Azurmendi, I. Agote, and E. Zuza, "A review on recent developments in binder jetting metal additive manufacturing: Materials and process characteristics," Powder Metall. **62**, 267 (2019).
[2]Y. X. Wang *et al.*, "Overview of 3D additive manufacturing (AM) and corresponding AM composites," Composites A **139**, 106114 (2020).

[3]N. Lazarus and H. H. Tsang, "3-D printing structural electronics with conductive filaments," IEEE Trans. Compon. Packaging Manuf. Technol. **10**, 1965 (2020).
[4]F. Tavakoli, S. H. Davis, and H. P. Kavehpour, "Spreading and arrest of a molten liquid on cold substrates," Langmuir **30**, 10151 (2014).
[5]R. de Ruiter *et al.*, "Contact line arrest in solidifying spreading drops," Phys. Rev. Fluids **2**, 043602 (2017).
[6]S. Schiaffino and A. A. Sonin, "Motion and arrest of a molten contact line on a cold surface: An experimental study," Phys. Fluids **9**, 2217 (1997).
[7]R. Herbaut *et al.*, "A criterion for the pinning and depinning of an advancing contact line on a cold substrate," Euro. Phys. J. Spec. Top. **229**, 1867 (2020).
[8]S. Schiaffino and A. A. Sonin, "Molten droplet deposition and solidification at low Weber numbers," Phys. Fluids **9**, 3172 (1997).
[9]S. Schiaffino and A. A. Sonin, "On the theory for the arrest of an advancing molten contact line on a cold solid of the same material," Phys. Fluids **9**, 2227 (1997).
[10]P. Kant, R. B. J. Koldeweij, K. Harth, and M. A. J. D. L. van Limbeek, "Fast-freezing kinetics inside a droplet impacting on a cold surface," PNAS **117**, 2788 (2020).
[11]M. V. Gielen *et al.*, "Solidification of liquid metal drops during impact," J. Fluid Mech. **883**, A32 (2020).
[12]L. Wang, W. Kong, F. Wang, and H. Liu, "Effect of nucleation time on freezing morphology and type of a water droplet impacting on cold substrate," Int. J. Heat Mass Transfer **130**, 831 (2019).
[13]Y. D. Shikhmurzaev, "Moving contact lines and dynamic contact angles: A 'litmus test' for mathematical models, accomplishments and new challenges," Eur. Phys. J. **229**, 1945 (2020).
[14]L. I. Rubenšteĭn, *The Stefan Problem* (American Mathematical Society, Providence, RI, 1971).
[15]C. Huh and L. E. Scriven, "Hydrodynamic model of steady movement of a solid/liquid/fluid contact line," J. Colloid Interface Sci. **35**, 85 (1971).
[16]Y. D. Shikhmurzaev, *Capillary Flows with Forming Interfaces* (Chapman & Hall/CRC, Boca Raton, Toronto, New York, 2007).
[17]J. W. Gibbs, *The Collected Works of J. Willard Gibbs* (Longmans, Green & Co., New York, 1928), Vol. 1.
[18]L. M. C. Sagis, "Dynamic behavior of interfaces: Modeling with nonequilibrium thermodynamics," Adv. Colloid Interface Sci. **206**, 328–343 (2014).
[19]A. I. Rusanov, "Surface thermodynamics revisited," Surf. Sci. Rep. **58**, 111 (2005).
[20]G. L. Buchbinder and P. K. Galenko, "Boundary conditions and heat resistance at the moving solid-liquid interface," Phys. A **489**, 149 (2018).
[21]R. Defay, I. Prigogine, and A. Bellemans, *Surface Tension and Adsorption* (Longmans, Green & Co., London, 1966).
[22]D. Bedeaux and S. Kjelstrup, "Fluid-fluid interfaces of multi-component mixtures in local equilibrium," Entropy **20**, 250 (2018).
[23]E. A. Guggenheim, "The thermodynamics of interfaces in systems of several components," Trans. Faraday Soc. **35**, 397 (1940).
[24]D. Bedeaux, A. M. Albano, and P. Mazur, "Boundary conditions and non-equilibrium thermodynamics," Phys. A **82**, 438 (1976).
[25]R. Caroli, C. Caroli, and B. Roulet, "Non-linear thermodynamics of the solidification problem," J. Cryst. Growth **66**, 575 (1984).
[26]L. I. Sedov, *Mechanics of Continuous Media* (World Scientific, Singapore, 1997), Vol. 1.
[27]Y. D. Shikhmurzaev, "The moving contact line on a smooth solid surface," Intl J. Multiphase Flow **19**, 589 (1993).
[28]J. E. Sprittles and Y. D. Shikhmurzaev, "Coalescence of liquid drops: Different models versus experiment," Phys. Fluids **24**, 122105 (2012).
[29]J. E. Sprittles and Y. D. Shikhmurzaev, "The coalescence of liquid drops in a viscous fluid: Interface formation model," J. Fluid Mech. **751**, 480 (2014).
[30]J. E. Sprittles and Y. D. Shikhmurzaev, "Finite element simulation of dynamic wetting flows as an interface formation process," J. Comp. Phys. **233**, 34 (2013).
[31]T. D. Blake and Y. D. Shikhmurzaev, "Dynamic wetting by liquids of different viscosity," J. Colloid Interface Sci. **253**, 196 (2002).
[32]T. D. Blake, M. Bracke, and Y. D. Shikhmurzaev, "Experimental evidence of nonlocal hydrodynamic influence on the dynamic contact angle," Phys. Fluids **11**, 1995 (1999).
[33]J. E. Sprittles and Y. D. Shikhmurzaev, "Finite element simulation of dynamic wetting flows as an interface formation process (vol 233, pg 34, 2013)," J. Comp. Phys. **274**, 936 (2014).
[34]H. W. Wilson, "XX. On the velocity of solidification and viscosity of supercooled liquid," Philos. Mag. **50**, 238 (1900).
[35]S. H. Davis, *Theory of Solidification* (Cambridge University Press, Cambridge, 2001).
[36]V. S. Ajaev and S. H. Davis, "The effect of tri-junction conditions in droplet solidification," J. Cryst. Growth **264**, 452 (2004).
[37]J. D. Martin, B. G. Hillis, and F. Hou, "Transition Zone Theory compared to standard models: Reexamining the theory of crystal growth from melts," J. Chem. Phys. C **124**, 18724 (2020).
[38]A. M. Karim, S. H. Davis, and H. P. Kavehpour, "Forced versus spontaneous spreading of liquids," Langmuir **32**, 10153 (2016).
[39]L. Gránásy *et al.*, "Phase-field modeling of polycrystalline solidification: From needle crystals to spherulites—A review," Metall. Mater. Trans **45**, 1694 (2014).
[40]L. Gránásy *et al.*, "Phase-field modeling of crystal nucleation in undercooled liquids—A review," Progr. Mater. Sci. **106**, 100569 (2019).
[41]Y. D. Shikhmurzaev, "Moving contact lines in liquid/liquid/solid systems," J. Fluid Mech. **334**, 211 (1997).
[42]C. C. Templeton, "Oil-water displacement in microscopic capillaries," Trans. AIME **8**, 211 (1956).
[43]C. N. C. Lam *et al.*, "The effect of liquid properties to contact angle hysteresis," Colloid Surf. A **189**, 265 (2001).
[44]C. N. C. Lam *et al.*, "Study of the advancing and receding contact angles: Liquid sorption as a cause of contact angle hysteresis," Adv. Colloid Interface Sci. **96**, 169 (2002).